Influence of facade materials on runoff due to wind-driven rain

Van den Brande Thijs [1], Teblick Leen [1], Blocken Bert [2], and Roels Staf [1]

[1]*Builing Physics Section, KU Leuven, Kasteelpark Arenberg 40 – bus 2447, B-3001 Leuven, Belgium*
[2]*Building Physics and Services, Department of the Built Environment, Eindhoven University of Technology, Eindhoven, The Netherlands*

Keywords: Wind-driven rain, runoff, absorption, HAM, numerical modelling

ABSTRACT

As wind-driven rain is one of the most important moisture sources for a building envelope, a reliable prediction of the wind-driven rain load is a prerequisite to assess the durability of building facade components. To incorporate wind-driven rain in HAM models (heat, air and moisture), many factors should be taken into account. Not only building geometry, wind speed and wind direction, raindrop size distribution, etc. influence the rain load on buildings, but also phenomena such as raindrop impact, absorption, evaporation and runoff should be taken into account. The latter phenomena are however not yet incorporated in the current HAM-models. The present study focuses on the runoff and absorption of wind-driven rain on building facades. It couples a simplified runoff model with a HAM model. In a first part of this study, the model is briefly described. In the second part, the model is used to calculate the amount of runoff due to wind-driven rain during a two-shower rain event on different facade materials. The catch ratio distribution, previously calculated with the use of computational fluid dynamics, was combined with weather data, on a 10-minute basis, from Leuven, Belgium to obtain the total amount of rain water supplied to the building surface. The rain water which cannot be absorbed by the material is used as an input for the runoff module in the HAM-program. It is found that, depending on the material, runoff of wind-driven rain can be a significant moisture source for underlying envelope parts.

1. Introduction

Moisture in porous building materials poses an important problem for the durability of the construction. It contributes to damage due to freeze-thaw cycles, biological damage such as fungal and mould growth, surface soiling, both dirty- and white washing of facades (Küntz and van Mier 1997, Etyemezian et al. 2000), leaching of nanoparticles into the environment (Kaegi et al. 2008, 2010),… Of all moisture sources for the building envelope, wind-driven rain is the most important one (Karagiozis et al. 1997, Blocken and Carmeliet 2004). It is therefore important to assess the impact of the wind-driven rain load when analysing moisture problems of building envelopes.

Although the commonly used HAM models are extensively elaborated and most of them now take the amount of wind-driven rain on building facades into account, secondary effects of rain, such as splashing and bouncing of raindrops (Abuku et al., 2009a) and the runoff of moisture along the surface, have not yet been implemented. This study tries to incorporate the secondary phenomenon of runoff in a previously developed HAM model. As an input for the simulation model, the amount of wind-driven rain is needed. In the past decades, much attention has been attributed to the calculation of the wind-driven rain (WDR) on building facades. An overview is given in Blocken and Carmeliet (2004). Runoff occurs whenever the moisture supply due to WDR exceeds the possible amount of absorbed moisture at the material surface. In the commonly used HAM-models, the modelling of moisture flow is based on capillary pressure or moisture content with a moisture flow at the boundary. When saturation is reached, the driving potential is set to a constant value and the surplus moisture flows are disregarded (e.g. Janssen et al. 2007).

On the other hand, liquid film flow has been extensively studied in other disciplines than building physics, such as chemical engineering and biology. Several models to calculate runoff have been developed and evaluated in the past (e.g. Ruyer-Quil and Manneville 1998, 2000; Moran et al. 2002; Kondic and Diez 2004). In building physics however, the coupling between fluid flow on a surface and the hygrothermal behaviour of the wall has, to the authors' knowledge, only been made by Blocken et al. (2002) and Blocken and Carmeliet (2012), who used a very simplified rain absorption model. In the first step of this study, we incorporate runoff of rain water in a HAM model. To do so, the Nusselt solution for fluid flow on an inclined plane was coupled to the HAM model "HAMFEM". For this paper the model developed by Janssen et al. (2007) is used.

In the first part of this paper, the simulation models used to calculate the water film at the envelope's surface and the moisture transfer inside the building element are briefly described. The second part of the paper consists of a simple example to explain the methodology. Finally, some conclusions and remarks are made on which further investigation can be based.

2. Numerical model

The simulations in this study were conducted with the finite element HAM-model HAMFEM, developed by the Building Physics Section of the K.U.Leuven (Janssen et al. 2007). The original HAM-code was extended with a module to calculate the runoff of rainwater on the exterior surface of the building envelope. Both models are solved alternately by using staggered solution procedures and use each other's results as input (Fig. 1).

2.1 HAMFEM model

The HAM-model used in this study is a finite element model based on the standard partial differential equations of coupled heat, air and moisture transfer in porous building materials (Hagentoft et al. 2004). Because the focus of this study is on moisture transport, the temperature and air

transfer equations are not included here. The moisture transfer in the material is governed by Eq. (1).

$$\xi \rho_0 \frac{\partial p_c}{\partial t} + \nabla(q_{ext}) = 0 \quad (1)$$

In this equation, ξ represents the moisture capacity (kg/m³.Pa), i.e. the derivative of the moisture retention curve, ρ_0 is the dry density of the material (kg/m³), p_c stands for capillary pressure and t for the time. ∇ is the divergence operator and q_{ext} is the moisture flow rate (kg/m².s) at the surface.

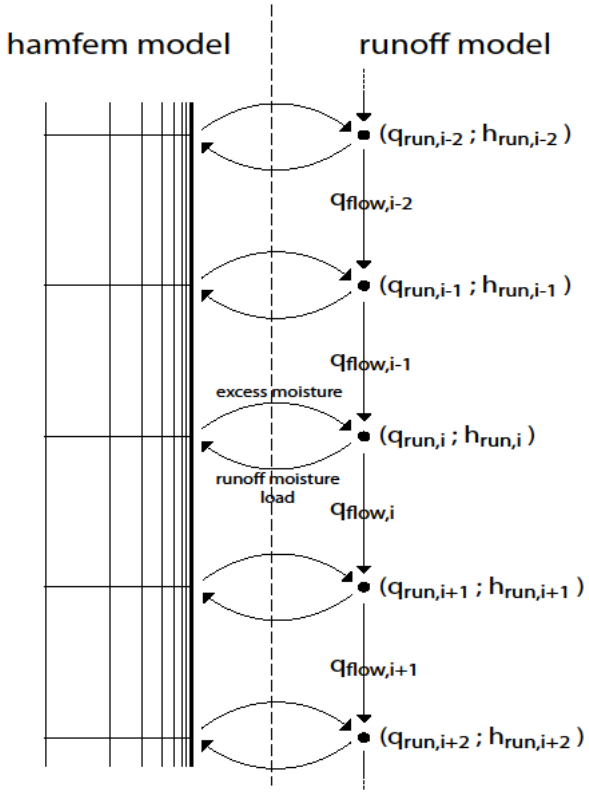

Fig. 1. Schematic representation of the coupled HAMFEM-runoff model. HAMFEM uses the amount of water in the runoff layer ($q_{run,i}$) for input and returns the excess moisture that is used by the runoff model. The amount of vertical flow ($q_{flow,i}$) and the height of the layer ($h_{run,i}$) are used to evaluate the layer.

The moisture supply from the environment (q_{ext}) originally consists of two terms: moisture supply due to rain (q_{wdr}) and evaporation due to unequal vapour pressure between material and the surrounding air (q_{evap}) and is defined by Eq. (2):

$$q_{ext} = q_{wdr} + \beta\left(p_{v,a} - p_{v,surf}\right) \quad (2)$$

In which β is the surface vapour transfer coefficient (s/m), $p_{v,a}$ the vapour pressure in the air and $p_{v,surf}$ the vapour pressure at the surface of the building envelope part (both in Pa). Concerning the absorbed moisture flow q_{abs}, as long as the moisture content at the surface remains below the capillary moisture content, the moisture flow into the material is equal to the flow due to wind-driven rain (q_{ext}). From the moment capillary saturation is attained (the moment the moisture supply at the boundary exceeds the possible inflow into the material), the moisture flow into the material reduces to $k\frac{\partial p_c}{\partial \mathbf{n}}$, in which k is the liquid moisture permeability (s) and $\mathbf{n}$ is the vector normal to the surface. At this moment, the capillary pressure at the surface is set to 0 Pa in the model. This results in the following equation:

$$q_{abs} = \max(q_{ext}, k\frac{\partial p_c}{\partial \mathbf{n}}) \quad (3)$$

As in most HAM models, this excess moisture was discarded from the calculations by the original HAM model. In the present study, the model is extended with a runoff module that uses the excess moisture to calculate the liquid film flow at the surface and the amount of runoff (Fig. 2). As a consequence, the runoff layer can be a supplementary moisture supply to the wall. When a water film appears at the surface, the total moisture supply from the environment in Eq. (2) will be extended with a third term q_{runoff} to incorporate the supplementary supply due to water runoff:

$$q_{ext} = q_{wdr} - q_{evap} + q_{runoff} \quad (4)$$

2.2 Runoff model

For the runoff model, the so called Nusselt solution is used (Ruyer-Quil and Manneville 1998, Blocken et al. 2002). It describes a steady parallel flow with a parabolic velocity profile. The Nusselt solution for fluid flow is a good first approximation, validated experimentally by Huppert (1982). Although some assumptions have to be made when using it. First, the liquid film should be thin enough for the Reynolds number to be small. At higher Reynolds numbers, the film becomes unstable and that cannot be taken into account by the model. On the other hand, the film should be thick enough to minimize the influence of surface forces. Furthermore, the Nusselt solution only accounts for incompressible Newtonian fluids with a negligible surface tension, surrounded by air with zero density and viscosity. To take surface tension into account, the general equation provided by Greenspan (1978) has to be used. Finally, the pressure is presumed to be constant over the film thickness. Taking into account the results from Fan et al. (2011), the shearing air flow close to the facade is not large enough to initiate the motion of the liquid sheet. In the simulations, only the two-dimensional case is considered. As a consequence, the formation of the typical “fingering pattern” on a facade due to the instability of the moisture front, could cannot yet be taken into account. The coordinate system used in the following equations, is depicted in Fig. 2. The thickness of the liquid film flowing down the facade is represented by the partial differential equation Eq. (5) below:

$$\frac{\partial h}{\partial t} + \frac{\rho g h^2}{\mu}\frac{\partial h}{\partial y} - \frac{(q_{wdr} - q_{abs} - q_{evap})}{\rho} = 0 \quad (5)$$

where h is the thickness of the film (m), ρ is the density of water (kg/m³), g is the gravitational constant (9.81 m/s²), μ is the dynamic viscosity of water (kg/m.s), t is the time and y represents the vertical distance along the wall surface. q_{wdr}, q_{abs} and q_{evap} are the moisture flows at the surface due to wind-driven rain, absorption and evaporation, respectively.

The solution to the equation is found by using a forward discretisation scheme in time and a backward scheme in space. This results in Eq. (6) for the film thickness:

$$h_i^{n+1} = h_i^n + \Delta t^{n+1}\left(\frac{q_{wdr}^{n+1} - q_{abs}^{n+1} - q_{evap}^{n+1}}{\rho} - \frac{\rho g}{3\mu}\left(\frac{(h_i^n)^3 - (h_{i-1}^n)^3}{\Delta y_{i-1}}\right)\right) \quad (6)$$

In this equation, n represents the time step and i is the number of the surface node.

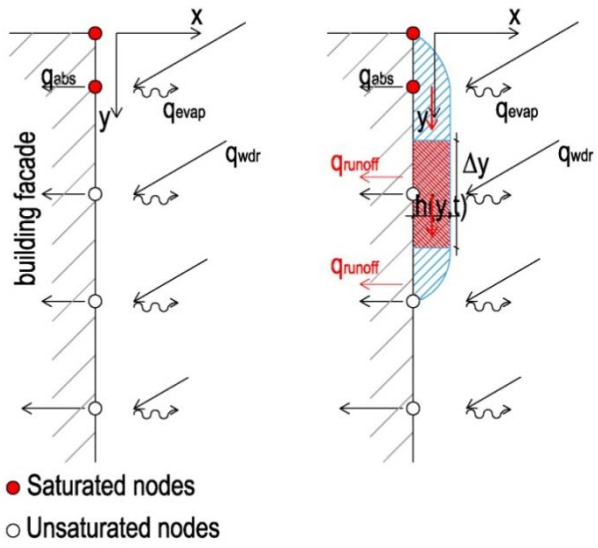

Fig. 2. Coordinate system and incoming flows of the coupled runoff model and HAM-model.

The amount of moisture running down from node *i* is represented by the flow rate given by Eq. (7) that results from the Nusselt solution:

$$q_{flow,i} = \frac{\rho}{\Delta y_i}\int_0^h v\,dx = \frac{\rho^2 g h^3}{\Delta y_i 3\mu}\ \left[\frac{kg}{m^2.s}\right] \quad (7)$$

in which *v* is the flow velocity in the vertical direction. This gives the opportunity to calculate the moisture flow at the boundary (q_{runoff}) using Eq. 8.

$$q_{runoff} = \frac{\Delta h * \rho_l}{\Delta y} + q_{flow,i-1} - q_{flow,i} \quad (8)$$

In which Δy is the height of a cell represented by node *i* and $q_{run,i-1}$ and $q_{run,i}$ are the film flow rate as defined in Eq. (7) in the node above the considered node and the node itself, respectively.

3. Simulation example

3.1 Materials

Simulations were conducted for two types of wall finishing and one rain event. The considered wall panel had a thickness of 2 cm and a height of 10 m. One panel was made of concrete, the other of brick. The moisture characteristics of both materials were taken from Hagentoft et al. (2004).

3.2 Boundary and initial conditions

Two simulation runs for each material were conducted for this study. Both runs are based on boundary conditions taken from measurements at the VLIET building of the Building Physics Section in Leuven. The data were available at a 10-minute basis, which is about the maximal time step for wind-driven rain measurements to be valuable (Blocken & Carmeliet 2007). The rain event consists of a one-hour period in which two short rain spells occur and with only small deviations in relative humidity (Rh_e) and temperature (T_e). The horizontal rain intensity (R_h) is different for both spells. The average of the wind speed (U_{10}) and wind direction (θ) during the simulation were 5 m/s and 200.8° from North, respectively. The orientation of the facade that is simulated is chosen perpendicular on the average wind direction. The average relative humidity was 92.4%. The moisture transfer coefficient at the boundary (β_e) was kept constant. At the beginning of the simulation, the initial conditions of the wall were set at the average temperature and relative humidity. At the back side of the panel, neither heat nor moisture exchange with the surroundings was considered. The micrometeorological boundary conditions are summarized in Table 1.

To calculate the amount of rain on the facade from this weather data, two situations are investigated. Case A represents the situation with a high moisture load at the top of a 10m wall and almost no moisture load below. This situation can be compared with some examples of bad design where rain, collected on large horizontal or glass surfaces, is not discharged properly and runs down the wall. The second case B represents a single 10x10x10 m³ tower building in a free-flow environment. The catch ratios were obtained from CFD simulations by Blocken and Carmeliet (2006). These catch ratios are a function of the wind speed and horizontal rain intensity and therefore depend on the particular rain event. This results in two graphs for the rain event with two showers that differ in both wind speed and rain intensity. The results for both situations for both the concrete and the brick wall will be discussed separately. The wind-driven rain catch ratios along the building facade for both situations are depicted in Fig. 3.

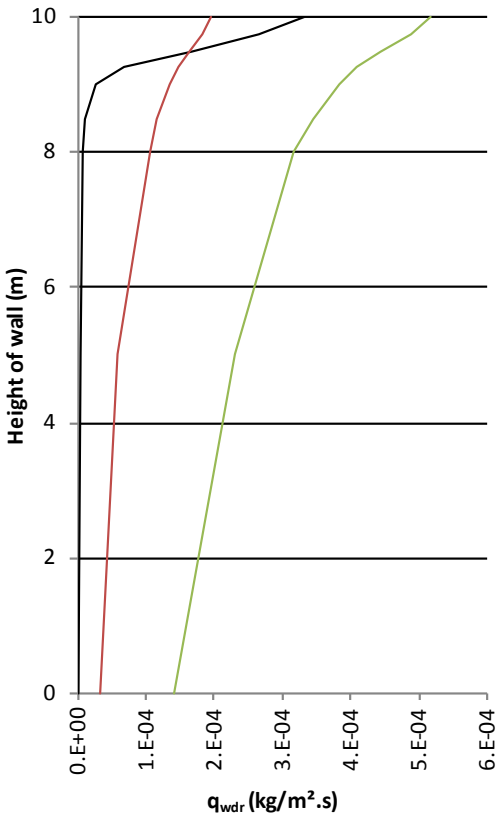

Fig. 3. Comparison of the wind driven rain from case A with case B, the catch ratios from Blocken en Carmeliet (2006) for a rain event with R_h = 1.2 mm/h and U_{10} = 4.1m/s and a rain event with R_h = 2.4 mm/h and U_{10} = 5.5 m/s.

Table 1. Micrometeorological boundary conditions for the simulations

Time	T_e [°C]	Rh_e [-]	R_h $[l/m^2h]$	U_{10} [m/s]	θ [° N]	β_e [s/m]
0-10 min	7.78	0.936	1.2	4.1	201.7	1.10^{-8}
10-20 min	8.04	0.924	0.0	4.8	198.6	1.10^{-8}
20-30 min	8.14	0.916	0.0	5.5	199.6	1.10^{-8}
30-40 min	8.24	0.913	2.4	5.5	194.5	1.10^{-8}
40-50 min	8.19	0.924	0.0	5.2	206.3	1.10^{-8}
50-60 min	8.19	0.929	0.0	5.0	204.4	1.10^{-8}

3.3 Results

In the following, the simulation results with and without the calculation of runoff are compared for the concrete panel and brick wall for the two different moisture load configurations. From the simulation without calculation of the moisture runoff, the amount of excess water can be deduced.

3.3.1 Case A: high moisture loads at the top

Using the wind driven rain distribution, defined in Fig. 3, high moisture loads are only present at the top of the concrete slab. The limited moisture capacity of concrete leads to quick saturation of the surface at the top with moderate amounts of wind-driven rain. In the following the results with and without including runoff will be discussed.

In Fig. 4a, the cumulative moisture flows during a one hour simulation are depicted without including runoff. It can be seen that the amount of excess water represents 42-62% of the supplied moisture load. This leads Janssen et al. (2007) to suspect that the excess moisture, which is disregarded by the current HAM-models, might be a significant moisture source for underlying building parts which are not yet saturated. When observing the simulation with calculation of the moisture film (Fig. 4b), it can be seen that the excess moisture is used for the formation of the runoff layer. When it stops raining, the film decreases by either evaporation or absorption, which fluxes are noticeably higher than in the case without surface film simulation.

The graph in Fig. 5 depicts the growth of the runoff layer during the first rain shower- of the event. The full lines represent the situation as long as it is raining (growth of the layer), the dotted lines the drying phase of the layer and the material. After about 5 seconds, the water layer on the surfaces starts to grow. From that moment, the supplied moisture can no longer be absorbed and the excess moisture, which was originally disregarded from the HAM-calculation, is used as an input of the runoff model. At first, the moisture layer mainly grows in the thickness direction and it does not yet run down the surface. When the maximum thickness is reached, the moisture layer starts to run down the facade, wetting the underlying locations on the surface. When it stops raining (after 600 s, dotted lines in Fig. 6), the moisture film runs down the facade while the surface layer remains saturated.

The influence of the runoff layer can also be seen when looking at the average moisture content of the wall (Fig. 6). As long as it rains, there seems to be hardly any difference between the moisture content of the wall with and without runoff layer. Once the runoff layer starts to flow a difference can be observed. When it stops raining, evaporation starts at places where no film is present. Without including runoff evaporation will occur across the whole surface of the wall, explaining the observed decrease of the average moisture content. The presence of the moisture film has two effects on the wall. First the film, running down towards unsaturated surface parts, is absorbed and the average moisture content of the concrete panel increases. Second, evaporation will take place at the surface of the moisture film and thus is not decreasing the moisture content in the wall.

Compared to the concrete slabs, no run-off layer is present in the case of a brick panel. Brick is able to absorb the wind-driven rain. This is shown in Fig. 7 where the supplied moisture load due to wind driven rain is completely absorbed. In time the supplied moisture evaporates from the brick. Larger moisture loads are needed to trigger runoff.

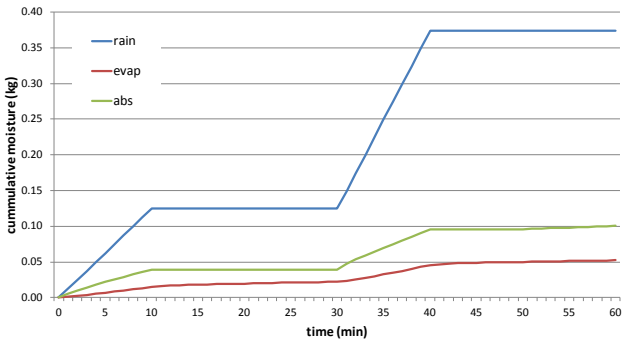

(a)

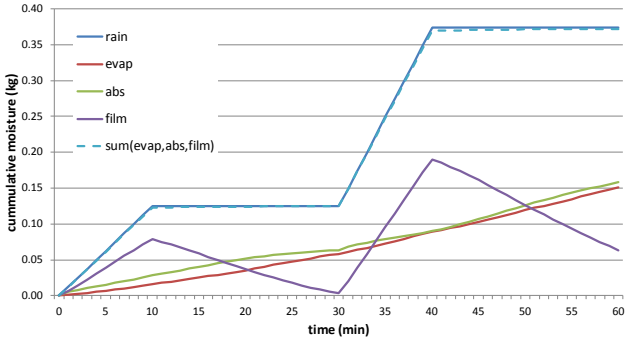

(b)

Fig. 4. Cumulative moisture flow on a concrete slab, without (a) and with (b) including runoff, during a 2 shower rain event for a concentrated moisture load at the top of the wall.

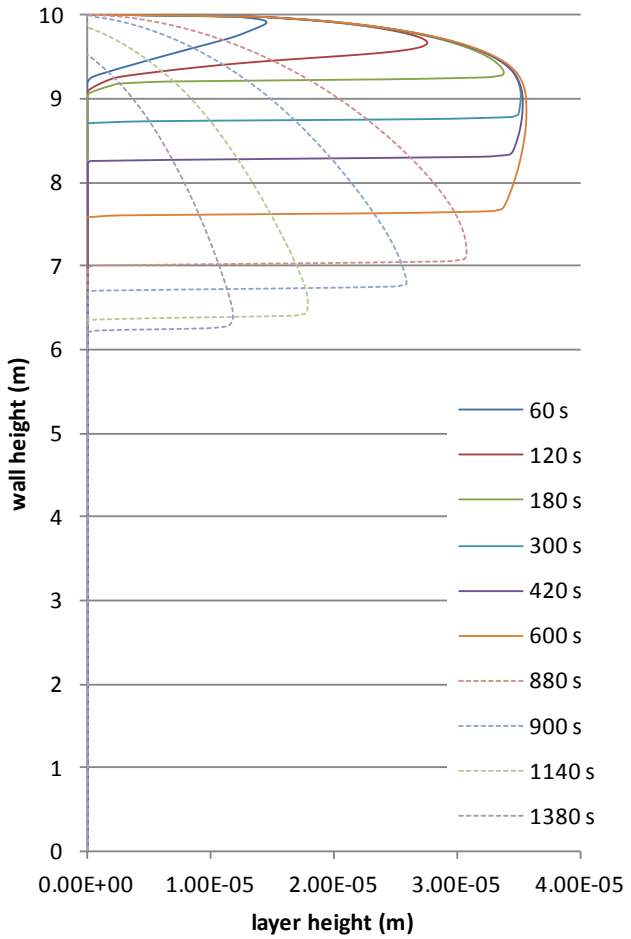

Fig. 5. Height of the runoff layer on a concrete wall during the first shower for a concentrated moisture load at the top of the wall. (full lines: growth of the layer, dotted lines: drying phase) at different stages.

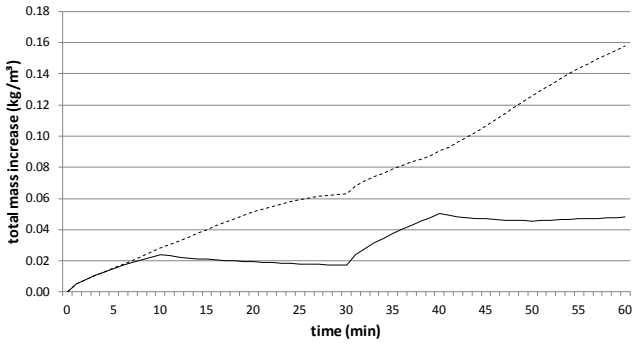

Fig. 6. Average moisture content of the concrete wall during a two shower rain event for a concentrated moisture load at the top of the concrete wall (dotted line: including runoff, full line: not including runoff).

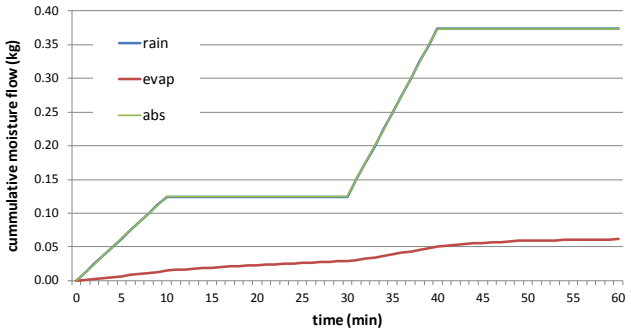

Fig. 7. Cumulative moisture flow on a brick wall during a two shower rain event for a concentrated moisture load at the top of the wall (case A).

3.3.2 Case B: Catch ratios calculated by Blocken and Carmeliet (2006)

With a more uniform distribution of the rain load saturation is reached at almost the same moment for the complete concrete slab. The limited moisture capacity of the first layer of material prohibits further absorption and a moisture film is formed over the complete height of the wall after a couple of seconds in the rain event. During the rain event, the moisture layer grows and runs down the surface to the bottom (Fig. 8). In the system without runoff 69% of the supplied moisture is discarded from the system. Compared to the simulations with runoff, where 63% of the supplied moisture runs to the bottom of the wall, one can notice a difference. The mass increase of the wall is higher than the amount of wind-driven rain that was discarded from the system. This is a result of the presence of the water film on the wall. In the case without including runoff, the drying phase immediately starts after the end of the shower event (after 10 minutes and after 40 minutes). In the case with runoff, drying only occurs when the water film disappeared due to runoff, absorption in to the material and evaporation at the surface of the film. The wetting stage lasts longer, thus resulting in higher moisture contents. During the first rain event no difference is noticed. This is illustrated in Fig. 9.

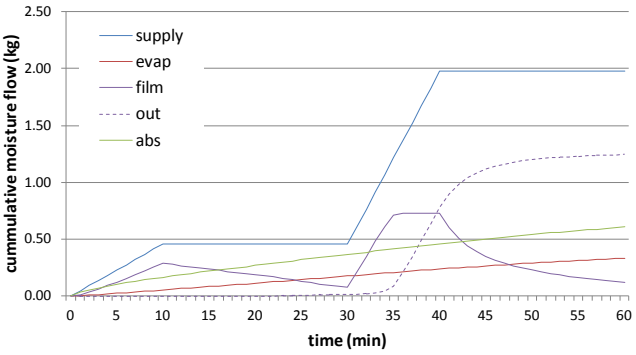

Fig. 8. Cumulative moisture flow on a concrete wall during a two shower rain event, including runoff, with catch ratios from Blocken and Carmeliet (2006).

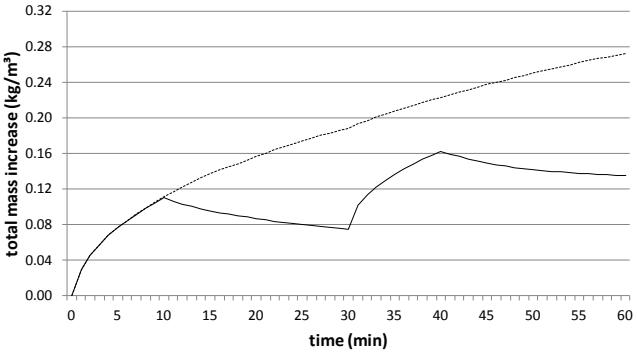

Fig. 9. Total mass increase of the wall during a two shower rain event with catch ratios from Blocken and Carmeliet (2006) with (dotted line) and without (full line) including runoff.

4. Conclusions

In this study, a model to simulate the runoff of excess moisture due to wind-driven rain on a building facade was shortly presented. The model was coupled with an existing HAM model developed by the Laboratory of Building Physics (HAMFEM).

It was found that the incorporation of a runoff model in the current HAM-models, influences the calculation of the moisture content of a wall. The influence is however greatly dependent on the boundary conditions and the material characteristics. For example, in case of the brick wall, no excess moisture appeared during the simulation.

However, in the first simulation of the concrete panel, with high moisture loads at the top of the wall, the increased moisture content represents 229% of the increase without including runoff, in the second simulation, with catch ratios from Blocken and Carmeliet (2006) only 202%. In the current HAM-models the excess moisture amount of water is disregarded from the calculation although the incorporation of runoff in the calculation results in a substantial increase of the average moisture content of a wall. The presence of a runoff layer delays drying during the first minutes after the rain event and results in an increased moisture flow towards areas that are not yet saturated. This indicates that, when one is interested in the influence of wind-driven rain on a building facade, it might be important to extend the current HAM models with a runoff calculation model.

In addition, when considered phenomena like surface soiling, it could be important to have an idea of the frequency at which runoff occurs and to incorporate also the third dimension and surface tension in the model to enable the calculation of the typical "fingering pattern" on wetted facades. When phenomena concerning deterioration are considered, it might be important to make long term assessments of the wall using measured weather data.

Acknowledgements

The results presented in this paper have been obtained in the framework of the research project FWO G.0448.10N, 'Strategies for moisture modelling of historical buildings in order to reduce damage risks', funded by the FWO-Flanders. The FWO-Flanders (Research Fund-Flanders) supports and stimulates fundamental research in Flanders (Belgium). Their financial contribution is gratefully acknowledged.

References

Abuku M., Janssen, H., Poesen J. & Roels S. 2009a. Impact, absorption and evaporation of raindrops on building facades. Building and Environment. 44[1]. pp. 113-124.

Abuku M., Janssen H. & Roels S. 2009b. Impact of wind-driven rain on historic brick wall buildings in a moderately cold and humid climate: Numerical analyses of moulds growth risk, indoor climate and energy consumption. Energy and Buildings. 41[1]. pp. 101-110.

Blocken B. & Carmeliet J. 2004. A review of wind-driven rain research in building science. Journal of Wind Engineering and Industrial Aerodynamics. 92[13]. pp. 1079-1130.

Blocken, B. & Carmeliet, J. 2006. The influence of the wind-blocking effect by a building on its wind-driven rain exposure. Journal of Wind Engineering and Industrial Aerodynamics. 94[2]. pp. 101-127.

Blocken B. & Carmeliet J. 2007. On the errors associated with the use of hourly data in wind-driven rain calculations on building facades. Atmospheric Environment, 41[11]. 2335-2343.

Blocken B., Janssen H. & Carmeliet J. 2002. On the modelling of runoff of driving rain on a capillary active surface. Proceedings of the 11th Symposium of Building Physics, Dresden, Germany, pp. 400-408.

Blocken B. & Carmeliet J. 2012. A simplified numerical model for rainwater runoff on building facades: possibilities and limitations. Building and Environment, 53, 59-73.

Couper R.R. 1974. Factors affecting the production of surface runoff from wind-driven rain. Second International CIB/RILEM Symposium on moisture problems in buildings. Rotterdam, The Netherlands.

Etyemezian V., Davidson C.I., Zufall M., Dai W., Finger S., Striegel M. 2000. Impingement of rain drops on a tall building. Atmospheric Environment 34. pp. 2399-2412.

Fan, J., Wilson, M. C. T., & Kapur, N. (2011). Displacement of liquid droplets on a surface by a shearing air flow. Journal of colloid and interface science, 356(1), pp. 286-92.

Greenspan H.P. 1978. On the motion of a small viscous droplet that wets a surface. Journal of Fluid Mechanics. 84[1]. pp. 125-143.

Hagentoft C.-E., Kalagasidis A.S. & Adl-Zarrabi B. 2004. Assessment method of numerical prediction models for combined heat, air and moisture transfer in building components: Benchmarks for one-dimensional cases. Journal of Building Physics. 27[4]. pp. 327-352.

Huppert, H. (1982). Flow and instability of a viscous current down a slope. Nature, 300, pp. 427-429.

Janssen H., Blocken B. & Carmeliet J. 2007. Conservative modelling of the moisture and heat transfer in building components under atmospheric excitation. International Journal of Heat and Mass Transfer. 50[5-6]. pp. 1128-1140.

Janssen H., Blocken B., Roels S. & Carmeliet J. 2007. Wind-driven rain as a boundary condition for HAM simulations: Analysis of simplified modelling approaches, Building and Environment 42[4]. pp. 1555-1567.

Kaegi R., Ulrich A., Sinnet B., Vonbank R., Wichser A., Zuleeg S., Simmler H., Brunner S., Vonmont H., Burkhardt M. & Boller M. 2008. Synthetic TiO_2 nanoparticle emission from exterior facades into the aquatic environment. Environmental Pollution. 156. pp. 233-239.

Kaegi R., Sinnet B., Zuleeg S., Hagendorfer H., Mueller E., Vonbank R., Boller M.& Burkhardt M. 2010. Release of silver nanoparticles from outdoor facades. Environmental Pollution. 158. pp. 2900-2905.

Karagiozis K., Hadjisophocleous G. & Cao S. 1997. Wind-driven rain distributions on two buildings. Journal of Wind Engineering and Industrial Aerodynamics. 67-68. pp. 559-572.

Kondic L. & Diez J. 2004. Instabilities in the flow of thin films on heterogeneous surfaces. Physics of Fluids. 16[9]. pp. 3341-3360.

Küntz M. & van Mier J.G.M. 1997. Field evidences and theoretical analysis of the gravity-driven wetting front instability of water runoffs on concrete structures. Heron. 42[4]. pp. 231-244.

Moran K., Inumaru J. & Kawaji M. 2002. Instantaneous hydrodynamics of a laminar wavy liquid film. International Journal of Multiphase Flow. 28. pp. 731-755.

Ruyer-Quil C. & Manneville P. 1998. Modeling film flows down inclined planes. The European physical journal B. 6[2]. pp. 277-292.

Ruyer-Quil C. & Manneville P. 2000. Improved modeling of flows down inclined planes. The European physical journal B. 15. pp. 357-369.